AMERICAN SOCIETY FOR MICROBIOLOGY | Molecular and Cellular Biology®

RESEARCH ARTICLE

VprBP/DCAF1 Regulates the Degradation and Nonproteolytic Activation of the Cell Cycle Transcription Factor FoxM1

Xianxi Wang,[a] Anthony Arceci,[a,b] Kelly Bird,[d] Christine A. Mills,[a,c] Rajarshi Choudhury,[a] Jennifer L. Kernan,[a,c] Chunxiao Zhou,[a,e] Victoria Bae-Jump,[a,e] Albert Bowers,[a,d] Michael J. Emanuele[a,b,c]

Lineberger Comprehensive Cancer Center, The University of North Carolina at Chapel Hill, Chapel Hill, North Carolina, USA[a]; Curriculum in Genetics and Molecular Biology, The University of North Carolina at Chapel Hill, Chapel Hill, North Carolina, USA[b]; Department of Pharmacology, The University of North Carolina at Chapel Hill, Chapel Hill, North Carolina, USA[c]; Eshelman School of Pharmacy, Division of Chemical Biology and Medicinal Chemistry, The University of North Carolina at Chapel Hill, Chapel Hill, North Carolina, USA[d]; Division of Gynecologic Oncology, The University of North Carolina at Chapel Hill, Chapel Hill, North Carolina, USA[e]

ABSTRACT The oncogenic transcription factor FoxM1 plays a vital role in cell cycle progression, is activated in numerous human malignancies, and is linked to chromosome instability. We characterize here a cullin 4-based E3 ubiquitin ligase and its substrate receptor, VprBP/DCAF1 ($CRL4^{VprBP}$), which we show regulate FoxM1 ubiquitylation and degradation. Paradoxically, we also found that the substrate receptor VprBP is a potent FoxM1 activator. VprBP depletion reduces expression of FoxM1 target genes and impairs mitotic entry, whereas ectopic VprBP expression strongly activates a FoxM1 transcriptional reporter. VprBP binding to CRL4 is reduced during mitosis, and our data suggest that VprBP activation of FoxM1 is ligase independent. This implies a nonproteolytic activation mechanism that is reminiscent of, yet distinct from, the ubiquitin-dependent transactivation of the oncoprotein Myc by other E3s. Significantly, VprBP protein levels were upregulated in high-grade serous ovarian patient tumors, where the FoxM1 signature is amplified. These data suggest that FoxM1 abundance and activity are controlled by VprBP and highlight the functional repurposing of E3 ligase substrate receptors independent of the ubiquitin system.

KEYWORDS cell cycle, cullin ring ligase, FoxM1, transcriptional regulation, ubiquitination

Received 11 November 2016 **Returned for modification** 29 November 2016 **Accepted** 10 April 2017

Accepted manuscript posted online 17 April 2017

Citation Wang X, Arceci A, Bird K, Mills CA, Choudhury R, Kernan JL, Zhou C, Bae-Jump V, Bowers A, Emanuele MJ. 2017. VprBP/DCAF1 regulates the degradation and nonproteolytic activation of the cell cycle transcription factor FoxM1. Mol Cell Biol 37:e00609-16. https://doi.org/10.1128/MCB.00609-16.

Address correspondence to Michael J. Emanuele, emanuele@email.unc.edu.

Changes in gene expression combined with targeted protein degradation dynamically shape the protein landscape. Gene expression is coordinated by transcription factors that specify genes for activation and cofactors that modulate transcription factor activity or alter the local chromatin environment. Posttranslational modifications (PTMs) play a crucial role in transcriptional dynamics. Phosphorylation, acetylation, methylation, and ubiquitylation of histone proteins are well studied and contribute significantly to gene expression dynamics (1). Similarly, posttranslational modification of transcription factors plays an important role in regulating genome output.

FoxM1 is an oncogenic, cell cycle-regulated transcription factor that was discovered as both a marker and a key mediator of cell proliferation (2–4). Subsequent work clarified the importance of FoxM1 in proliferation through its role in cell cycle progression (reviewed in reference 5). FoxM1 controls the mitotic transcriptional program, and its depletion significantly impairs normal mitotic entry and progression (6–9). In addition, FoxM1 and its transcriptional network have been associated with numerous cancers (5, 10). Notably, FoxM1 is the key regulator of a proliferative gene expression signature found in high-grade serous ovarian cancer (HGSOC), basal-like breast cancers,

and uterine serous carcinomas (11–13). In HGSOC, the FoxM1 signature is upregulated in nearly 90% of patient tumors (12).

FoxM1 activity peaks in G_2/M phase, consistent with its role in dictating mitotic gene expression, and several kinases have been implicated in its activation (6, 14–18). FoxM1 is repressed by an intramolecular interaction with its amino-terminal domain, and this inhibition is relieved by cyclin-dependent kinase (CDK) phosphorylation (19). In addition, the cell cycle kinases MELK and PLK1 can activate FoxM1 (20–24).

In addition to phosphorylation, posttranslational addition of ubiquitin is utilized to control gene expression. The oncogenic transcription factor c-Myc highlights the complex role that ubiquitin plays in transcriptional regulation (25). Myc is targeted for proteolysis by several E3 ubiquitin ligases, including a Skp1-, cullin 1-, F-box-containing complex (SCF)-type cullin ring ligase (CRL) and the substrate receptor Skp2 (SCF^{Skp2}) (26, 27). Whereas protein ubiquitylation and degradation are most often considered inactivating events, unexpectedly, Skp2 activates Myc-dependent transcription (26, 27). Ubiquitylation-dependent activation of Myc is further borne out by studies using a lysine-less version that cannot be ubiquitylated and is deficient in activating transcription (28). The role of ubiquitylation in transcriptional activation builds on pioneering studies on the VP16 transcription activation domain whose activation in yeast requires an SCF ligase together with its substrate receptor Met30 (29). Furthermore, the ability of the ubiquitin machinery to activate transcription is corroborated by regulation of the human estrogen receptor (ERα) and its coactivator, SRC-3/AIB1, whose degradation is coupled to activation (29–32). Together, these studies highlight the complex role that ubiquitin plays in transcriptional control.

The role of ubiquitin ligases in activating FoxM1 has not been studied. We recovered FoxM1 in a global screen for substrates of the modular CRLs, which represent the largest E3 ligase family in humans (33). CRL assembly is based on a common molecular scaffold and relies on a cullin backbone that simultaneously engages substrates and E2 ubiquitin-conjugating enzymes. Cullin 4-based ligases (CRL4) use either of two highly related cullin proteins, Cul4A or Cul4B, that bind to the triple-β-propeller protein DDB1. Substrate receptor subunits bind directly to DDB1 and simultaneously recruit specific proteins to the enzyme complex for ubiquitylation (schematic in Fig. 1A) (34). Human Cul4A and Cul4B are highly similar (75% amino acid similarity); however, Cul4B has an amino-terminal extension and localizes exclusively to the nucleus, whereas Cul4A is both nuclear and cytoplasmic (35). Importantly, CRL4 function has been linked to chromatin regulation, cell cycle, viral infection, and the DNA damage response (34).

More than 50 CRL4 substrate receptors, termed DCAFs or DWD proteins (DDB1- and Cul4-associated factors; DDB1 binding WD40 proteins), have been identified (36–38). VprBP/DCAF1 is a nucleus-localized CRL4 substrate receptor named for its ability to bind the HIV accessory protein Vpr (and Vpx) following viral infection (39). Ectopic Vpr expression in human cells triggers a G_2 arrest that is dependent on $CRL4^{VprBP}$ (reviewed in reference 40). Significantly, VprBP associates with chromatin only during the G_2/M phase of the cell cycle (41). Knockout of VprBP in mice causes embryonic death prior to embryonic day 7.5 (E7.5), and conditional inactivation of VprBP in mouse cells or depletion using RNA interference (RNAi) in human cells produces cell cycle defects (41). Despite its importance in cell cycle control and development, $CRL4^{VprBP}$ has few known substrates and it remains unclear how it contributes to cell cycle progression. Endogenous $CRL4^{VprBP}$ substrates include the methylcytosine dioxygenase Tet2 (42) and the replication regulator Mcm10 (43). Other proteins are targeted for ubiquitylation only in response to HIV infection and include the phosphohydrolase SamHD1 (44). VprBP has been linked to the NF2 tumor suppressor and YAP-dependent transcription, suggesting a role in transcriptional regulation and cancer (45). Here, we describe a role for VprBP in controlling both the degradation and the activation of FoxM1.

RESULTS

FoxM1 stability is regulated by $CRL4^{VprBP}$. Using a fluorescence-based genetic reporter system termed global protein stability profiling (GPS), we previously searched

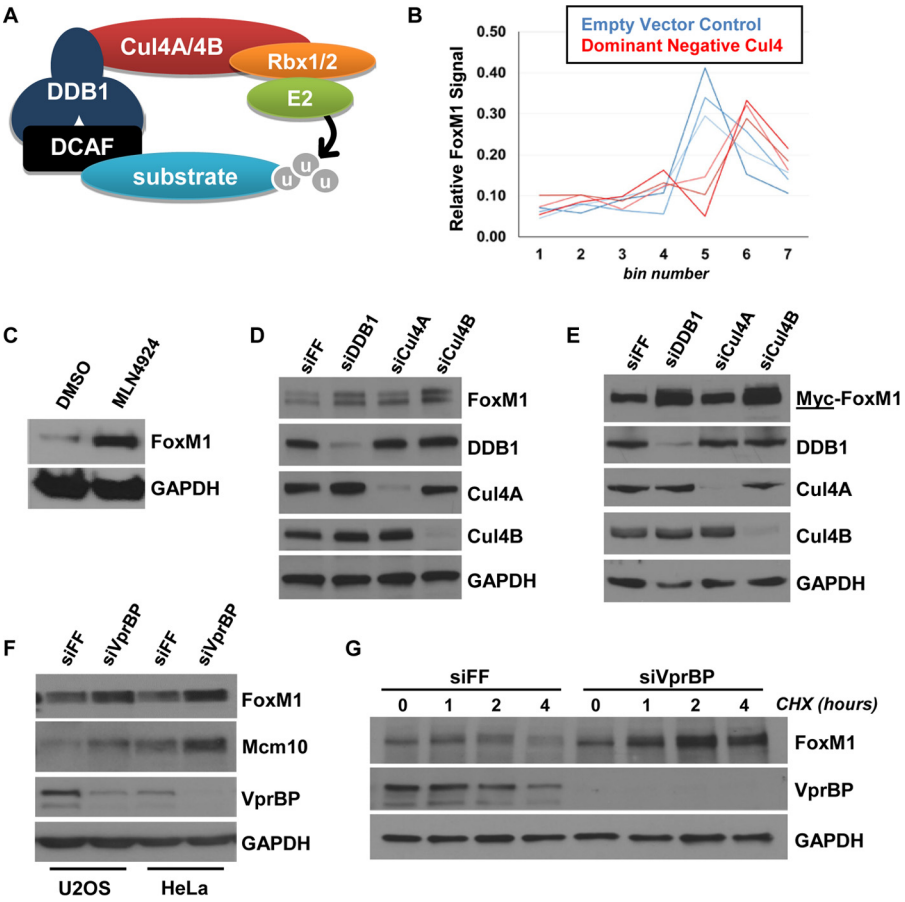

FIG 1 FoxM1 is regulated by Cul4, DDB1, and VprBP. (A) Illustration of the CRL4 complex. DDB1 bridges either Cul4A or Cul4B to substrate adaptor subunits termed DCAF or DWD proteins. Substrates are ubiquitylated by E2 enzymes that are recruited to the cullin backbone by Rbx1 or Rbx2. (B) FoxM1 scored in a GPS screen for CRL4 substrates. Three independent microarray probes were shifted in response to dominant negative Cul4 treatment. (C) U2OS cells treated with MLN4924 for 4 h and analyzed by immunoblotting. (D) U2OS cells were treated with siRNAs targeting FF (control), DDB1, Cul4A, or Cul4B and analyzed by immunoblotting after 72 h. (E) U2OS cells stably expressing Myc-FoxM1 were treated with siRNAs targeting firefly luciferase (FF), DDB1, Cul4A, Cul4B, or VprBP and analyzed by immunoblotting after 72 h. (F) U2OS and HeLa cells treated with siRNAs targeting FF or VprBP and analyzed by immunoblotting after 72 h. (G) U2OS cells treated with siRNAs targeting FF or VprBP were synchronized in S phase using thymidine. Cycloheximide was added 4 h after release into the cell cycle, and FoxM1 stability was analyzed by immunoblotting.

for substrates of the Cul4-based cullin ring ligase (CRL4) (33). The GPS expression system relies on a viral vector that expresses a bicistronic mRNA encoding both DsRed and an enhanced green fluorescent protein-open reading frame (EGFP-ORF) fusion protein. Using this system, we infer relative changes in the stability of EGFP-ORF fusions by examining the ratio between EGFP and DsRed fluorescence using flow cytometry. DsRed normalizes for expression of the reporter cassette on a single-cell basis. Using this system, we screened a pooled library of 293T cells expressing more than 13,000 individual EGFP-ORF fusion proteins (one ORF per cell). A schematic overview of the GPS screening system is depicted in Fig. S1 in the supplemental material and is described in detail elsewhere (33, 46).

To identify proteins whose stability is controlled by CRL4, we turned off the ligase by introducing a dominant negative construct targeting Cul4 and compared results under this condition to those obtained with a negative-control vector (33). GPS library cells from these two conditions were sorted into bins based on their EGFP/DsRed ratio using fluorescence-activated cell sorting (FACS). Genomic DNA (gDNA) was isolated from sorted cells in each bin, and ORFs were amplified from gDNA using PCR primers

designed against the viral backbone. Amplified ORF DNA was labeled and hybridized to custom-designed DNA microarrays containing multiple independent probes per gene. Quantifying the distribution of probe signals across bins allows us to infer changes in the stability of EGFP-ORFs (33). For example, a shift in the probe distribution to higher-numbered bins suggests that cells expressing a particular EGFP-ORF showed an increase in their EGFP/DsRed ratio, indicative of an increase in the stability of the EGFP-ORF fusion protein.

Three of the four probes corresponding to FoxM1 showed a shifted distribution after dominant negative Cul4 treatment, suggesting that EGFP-FoxM1 was stabilized by CRL4 inactivation (Fig. 1B). These three probes showed a highly consistent distribution across bins, suggesting that they accurately report the distribution of EGFP-FoxM1-expressing cells and that FoxM1 stability is regulated by CRL4.

To validate endogenous FoxM1 as a CRL substrate, we treated cells with MLN4924, a pharmacological small-molecule inhibitor that impairs CRL activation by interfering with the neddylation cascade (47). FoxM1 abundance was increased after a 4-h MLN4924 treatment in both 293T and U2OS cells (Fig. 1C; see also Fig. S2A in the supplemental material). The slower-migrating, neddylated form of Cul4 was undetectable after MLN4924 treatment, showing that neddylation was impaired (Fig. S2A). We next determined if FoxM1 is regulated by Cul4. We treated cells with small interfering RNA (siRNA) targeting either Cul4A, Cul4B, or DDB1 or with control oligonucleotides targeting firefly luciferase (FF). Seventy-two hours after transfection, cells were harvested for immunoblotting. Depletion of DDB1 and Cul4B led to a reproducible increase in the abundance of endogenous FoxM1, whereas depletion of Cul4A had a weaker and less consistent effect (Fig. 1D). Consistently, depletion of DDB1 and Cul4B increases the abundance of Myc-FoxM1, which is stably expressed from a heterologous promoter, and again, Cul4A had no effect (Fig. 1E; the underlining corresponds to the antigen used for blotting, e.g., Myc-FoxM1). Taken together, these data suggest that FoxM1 stability is regulated by CRL4.

The two best-studied CRL4 substrate receptors implicated in cell cycle control are Cdt2 and VprBP. Cdt2 engages substrates through a degron embedded within a PCNA-interacting peptide motif (PIP-box) (48). However, FoxM1 lacks a PIP-box. We therefore depleted VprBP using siRNA and measured FoxM1 abundance by immunoblotting. Depletion of VprBP increased endogenous FoxM1, as well as the known substrate Mcm10, in both HeLa and U2OS cells (Fig. 1F).

FoxM1 is degraded in G_1 phase by the APC/C^{Cdh1} ubiquitin ligase (49, 50). To determine if VprBP regulates FoxM1 at other times during the cell cycle and to rule out the possibility that differences in FoxM1 abundance were due to changes in cell cycle progression, we treated U2OS cells with siRNA targeting VprBP and then synchronized cells using thymidine in accordance with a previously established protocol (51). Cells were harvested 0, 2, 4, and 6 h after release and analyzed by immunoblotting. FoxM1 was consistently increased in the VprBP-depleted cells (Fig. S2B), suggesting that VprBP regulates FoxM1 degradation and that the increase in FoxM1 abundance is independent of gross cell cycle changes. Two independent siRNA oligonucleotides targeting VprBP produced a similar increase in FoxM1 levels in S-phase-synchronized cells (Fig. S2C). Similarly, we synchronized HCT116 cells in early S phase, late S phase/G_2, and G_2/M phase using thymidine, thymidine block and release, and nocodazole, respectively. FoxM1 was increased in synchronized, VprBP-depleted cells, indicating that VprBP controls FoxM1 abundance, independent of its effect on the cell cycle (Fig. S2D).

Next, we measured FoxM1 stability/half-life in control and VprBP-depleted cells that were synchronized in S phase, 2 h after thymidine release. VprBP depletion increased FoxM1 stability after treatment with the protein synthesis inhibitor cycloheximide (CHX) (Fig. 1G). Interestingly, in both control and VprBP-depleted cells, FoxM1 levels transiently increased after the addition of CHX. This is a highly reproducible result observed across several experiments. The acute increase in FoxM1 is evident in otherwise-untreated cells after the addition of CHX (Fig. S2E). While the mechanism underlying

this phenomenon remains unclear, it has long been appreciated that some proteins can increase following treatment with CHX (52).

FoxM1 interaction and ubiquitylation by VprBP. We next determined if VprBP binds to FoxM1 in HEK-293T cells transiently transfected with Myc-FoxM1 and hemagglutinin (HA)-VprBP to examine the possibility that FoxM1 is a direct $CRL4^{VprBP}$ substrate. Cells were treated with the proteasome inhibitor MG132 for 4 h prior to lysis and coimmunoprecipitation (co-IP) to promote the interaction between E3 ligase and substrate (53, 54). Following anti-HA-VprBP IP, we detected an interaction with FoxM1, and this interaction was enhanced by treatment with MG132 (Fig. 2A; see also Fig. S3A in the supplemental material). The interaction was also detectable when Myc-FoxM1 was immunoprecipitated (Fig. S3C). In addition, we precipitated endogenous FoxM1 from HEK-293T cell lysates and detected endogenous VprBP (Fig. 2B). Finally, we determined if FoxM1 and VprBP can directly interact. We immobilized bacterially purified 6×His-tagged FoxM1 (FoxM1-6His) on nickel-agarose beads and mixed them with purified, [^{35}S]methionine-labeled VprBP produced *in vitro* using purified transcription and translation machinery. VprBP bound to beads that had immobilized FoxM1-6His but was observed only in the flowthrough of control beads, strongly suggestive of a direct interaction (Fig. 2C).

To determine if VprBP can regulate FoxM1 ubiquitylation, we ectopically expressed 6His-ubiquitin in 293T cells with and without HA-VprBP. Cells were treated with MG132 prior to lysis in strong denaturing buffer (6 M guanidine–HCl), and 6His-ubiquitin conjugates were isolated on nickel-agarose. VprBP expression enhanced the ubiquitylation of endogenous FoxM1, measured by immunoblotting for FoxM1 (Fig. 2D). Likewise, VprBP significantly increased the ubiquitylation of ectopically expressed Myc-FoxM1 (Fig. 2E). Therefore, VprBP regulates the abundance, stability, and ubiquitylation of FoxM1.

To identify the domain in FoxM1 that interacts with VprBP, we synthesized a series of constructs encoding 160-amino-acid (aa) fragments of the FoxM1 protein spanning the length of its largest known open reading frame. We tested their ability to interact by expressing full-length HA-VprBP and Myc-FoxM1 fragments in HEK-293T cells and analyzing precipitates after anti-HA IP. A fragment of FoxM1 spanning amino acids 321 to 480 ($FoxM1^{321-480}$) interacted most strongly with VprBP (Fig. S3B). The same Myc-$FoxM1^{321-480}$ fragment bound to VprBP when Myc was precipitated (Fig. S3C). We conclude that the interaction between VprBP and FoxM1 is dependent on the region of FoxM1 spanning amino acids 321 to 480.

To identify a degron sequence motif in FoxM1, we examined molecular and structural data of a known VprBP substrate. SamHD1 is targeted by $CRL4^{VprBP}$ after HIV infection, and a ternary complex between VprBP, SamHD1, and the viral accessory protein Vpx has been crystallized (Fig. 2F) (55). Importantly, the amino acids in SamHD1 that mediate binding to VprBP and degradation have been mapped (55, 56). A segment between amino acids 615 and 625 in SamHD1 contributes significantly to VprBP binding, and several residues in this region are critical for its degradation (55, 56). We looked for matching sequences in FoxM1 between residues 321 and 480 and identified a region of similarity between residues 414 and 422 (Fig. 2F, bottom panel). We synthesized three mutant versions of the same region of aa 321 to 480, making amino acid substitutions that correspond to residues that we predicted would affect recognition by VprBP. These substitutions in FoxM1 included changes of RV to AA (aa 416 and 417), RI to AA (aa 418 and 419), and K to A (aa 422). We tested the ability of each version of the fragment to bind HA-VprBP by co-IP following treatment with proteasome inhibitors to normalize protein levels across IPs. We found that alanine substitutions at residues 418 and 419 (RI to AA) and 422 (K to A) impaired binding to VprBP (Fig. 2G). Notably, K622 in SamHD1, corresponding to K422 in FoxM1, directly contacts VprBP in the crystal structure and is required for SamHD1 degradation (55).

We next tested the stability of these fragments by CHX chase. Significantly, fragments that showed reduced binding also had higher basal expression (note that these

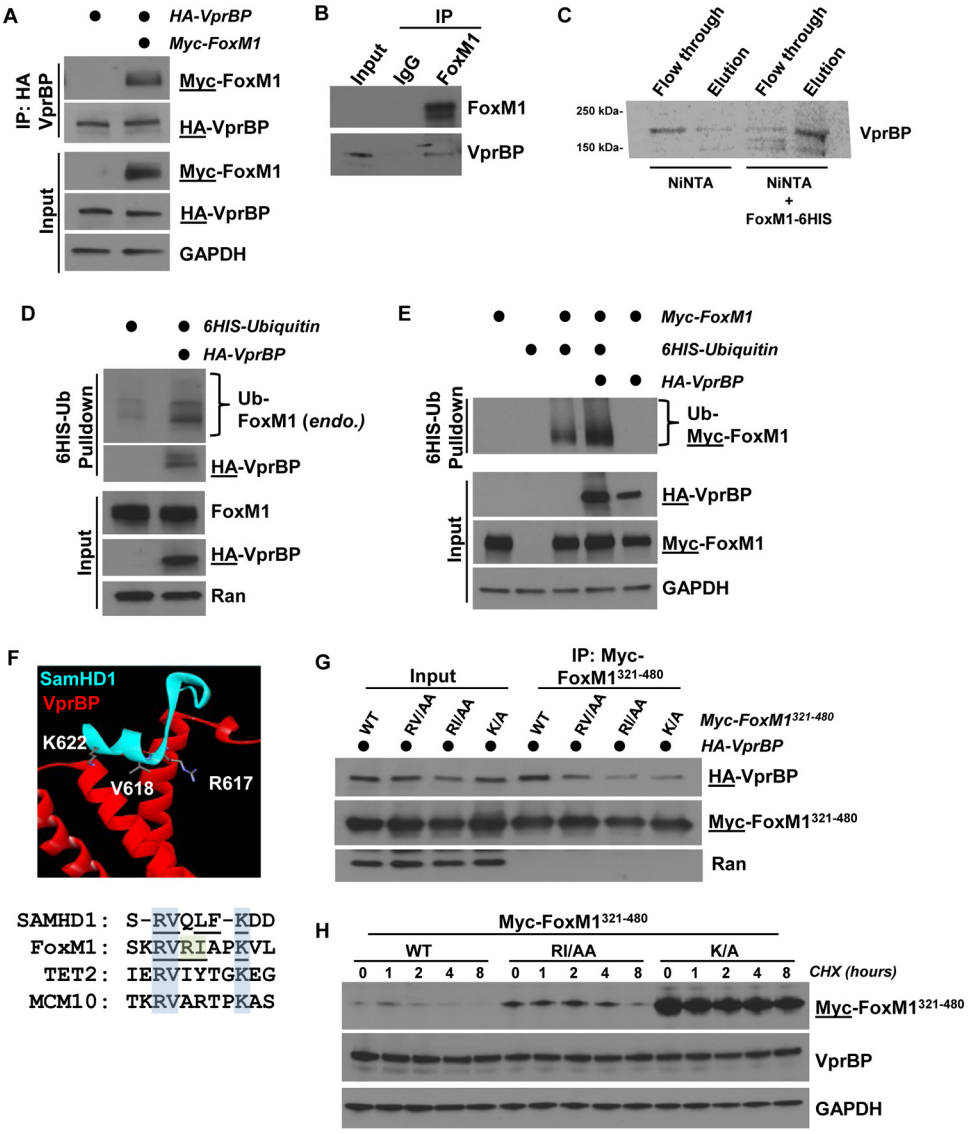

FIG 2 VprBP binds and ubiquitylates FoxM1 *in vivo*. (A) HA-VprBP and Myc-FoxM1 were transiently expressed in 293T cells. VprBP was recovered on anti-HA-agarose and analyzed by immunoblotting. Cells were treated with MG132 prior to lysis. (B) Endogenous FoxM1 was precipitated from a 293T cells extract and analyzed by immunoblotting. (C) Bacterially purified FoxM1-6His was incubated with *in vitro*-produced, [^{35}S]methionine-labeled VprBP. Flowthrough and eluates after pulldown were analyzed by autoradiography. (D and E) 6His-ubiquitin was transiently expressed in 293T cells with and without HA-VprBP. 6His-ubiquitin was recovered after lysis under strong denaturing conditions and analyzed by immunoblotting. Analysis of either endogenous (D) or exogenously expressed (E) Myc-FoxM1 was done by immunoblotting. (F) Crystal structure from Schwefel et al. (55) depicting the interaction between VprBP and SamHD1. Alignment of similar residues between SamHD1, FoxM1, and two other VprBP substrates (Tet2 and Mcm10) is shown below. (G) Amino acid substitutions were made in a FoxM1 fragment (aa 321 to 480) corresponding to the residues found in the VprBP-SamHD1 interface. Binding was analyzed as described for panel A between Myc-FoxM1$^{321-480}$ and HA-VprBP. (H) The stability of Myc-FoxM1$^{321-480}$ fragments that were impaired in their binding to VprBP was analyzed by CHX chase.

experiments were not done with proteasome inhibitors, in contrast to those whose results are shown in Fig. 2D) and increased stability relative to the wild-type (WT) fragment when expressed in 293T cells (Fig. 2H). We observed a similar increase in the stability of full-length FoxM1 when amino acids in the putative degron motif were changed (RVRIAPK to AAAAAPA; the half-life increased from 1.0 to 1.5 h). More-minor changes, specifically, K422A, similarly extended the half-life (Fig. S2F and G). These data are suggestive that this motif sequence, i.e., R-I/V-X-X-(X)-K, represents a putative VprBP degron. Similar sequences are found in established substrates Tet2 and Mcm10 (Fig. 2F) (42, 43).

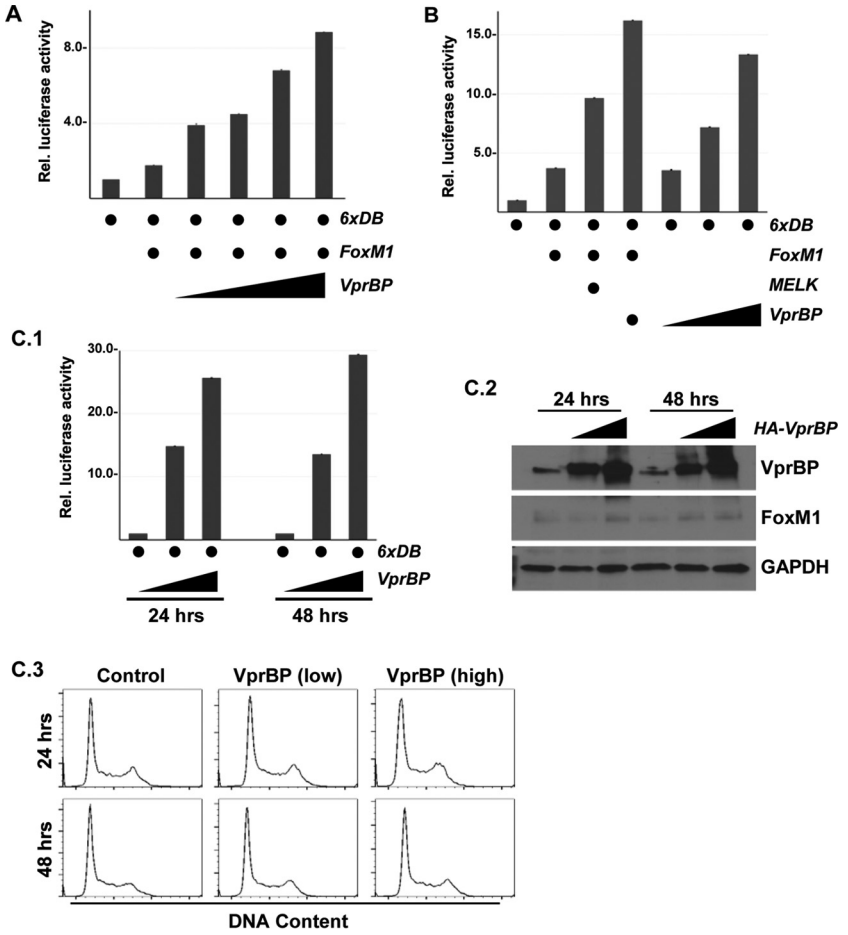

FIG 3 VprBP activates the FoxM1 6×DB transcriptional reporter. (A) FoxM1 and VprBP were expressed in 293T cells in combination with the 6×DB reporter. Luciferase activity was measured 48 h after transfection (error bars show standard deviations for technical triplicates). (B) Combinations of MELK, FoxM1, and VprBP were expressed in 293T cells with the 6×DB reporter. Luciferase activity was measured 48 h after transfection (error bars show standard deviations for technical triplicates). (C.1 to C.3) High and low concentrations of VprBP were expressed in 293T cells with the 6×DB reporter. At 24 and 48 h after transfection, identical populations of cells were measured for luciferase activity (C.1) and harvested and split for analysis by immunoblotting (C.2) and cell cycle analysis (C.3). Luciferase activity was measured (error bars show standard deviations for technical triplicates).

VprBP is a FoxM1 activator. To address the contribution of VprBP to FoxM1 activity, we utilized a well-characterized FoxM1 luciferase reporter construct (6×DB) (23). We measured reporter activity following transient expression of FoxM1 and VprBP in HEK-293T cells. Expression of FoxM1 increased reporter activity as expected (Fig. 3A). Remarkably, we also observed a strong, dose-dependent increase in reporter activity in response to VprBP when coexpressed with FoxM1 (Fig. 3A). We compared the ability of VprBP to activate FoxM1 to that of the known coactivator MELK (24). VprBP activated the reporter to a greater extent than MELK when transfected in equal amounts (Fig. 3B). Furthermore, VprBP activates the 6×DB reporter in the absence of ectopically expressed FoxM1 (Fig. 3B). We also measured the effect of VprBP on an unrelated luciferase reporter controlled by the oxidative stress response transcription factor Nrf2. FoxM1 and VprBP expression did not affect the Nrf2 luciferase reporter, whereas strong activation was achieved by Nrf2 expression (see Fig. S4A in the supplemental material).

We next expressed the 6×DB reporter with increasing amounts of VprBP and analyzed luciferase activity, cell cycle dynamics, and protein abundance all in the same experiment (Fig. 3C). VprBP activated reporter activity at both 24 and 48 h posttransfection in a dose-dependent manner (Fig. 3C.1). Importantly, the abundance of FoxM1

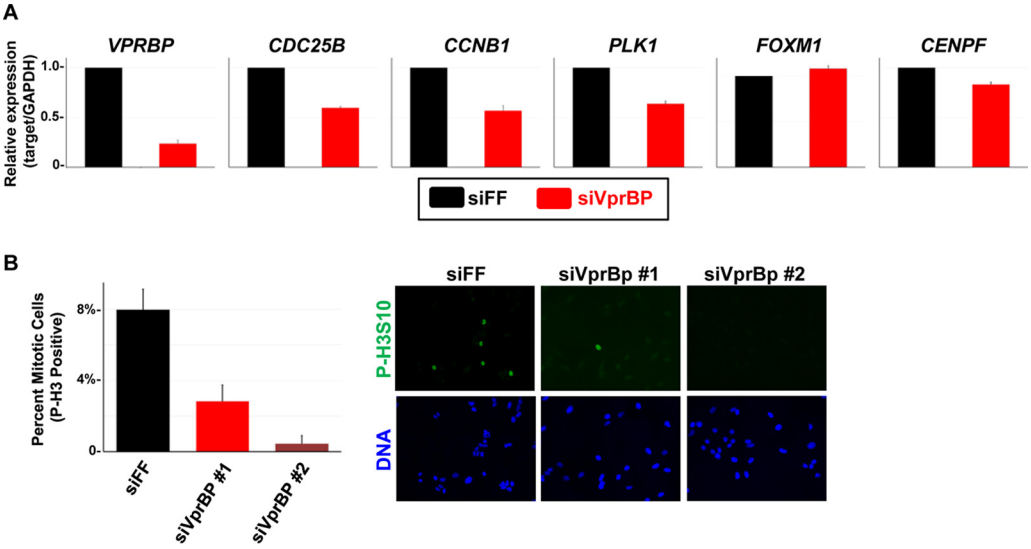

FIG 4 VprBP depletion reduces FoxM1 target gene expression and the number of mitotic cells. (A) U2OS cells treated with siRNAs targeting FF or VprBP were synchronized in G_2/M using a thymidine block and release. The expression of FoxM1 target genes was analyzed using RT-qPCR (error bars show standard deviations for technical triplicates). (B) U2OS cells treated with siRNAs targeting FF or VprBP were fixed and immunostained for phospho-histone H3 Ser10. DNA was counterstained with Hoechst stain. Images were captured using an automated imaging system, and the percentage of P-H3S10-positive cells was calculated from six wide-field images captured on an automated system. Representative images are shown.

remained unchanged at both time points and concentrations of VprBP (Fig. 3C.2). This demonstrates that the change in reporter activity is not due to changes in the overall level of FoxM1. It also suggests that VprBP does not activate FoxM1 by triggering its degradation, as is the case for Myc activation by Skp2 (26, 27). We examined the cell cycle using propidium iodide staining and analysis by flow cytometry and found no significant changes at either time point relative to controls (Fig. 3C.3). We therefore conclude that VprBP activates FoxM1 and that activation is independent of FoxM1 abundance and is not due to gross changes in cell cycle dynamics.

To directly interrogate the consequence of VprBP depletion on FoxM1 activity, we measured the transcript levels of FoxM1 target genes in synchronized U2OS cells (to alleviate cell cycle effects) that were depleted of VprBP. First, U2OS cells were synchronized in G_2/M following an 8-h release from thymidine block. The mRNA from control and VprBP-depleted cells was isolated, and FoxM1 target gene expression was measured using quantitative reverse transcription-PCR (RT-qPCR). The expression of several FoxM1 target genes was reduced in VprBP-depleted cells, including *CDC25B*, *CCNB1*, *PLK1*, and *CENPF* (Fig. 4A). The expression of VprBP was reduced by siRNA treatment as expected; however, the level of FoxM1 mRNA was unchanged. We performed a similar experiment by treating the cells with siRNA targeting FF, FoxM1, and VprBP and then blocking cells in mitosis with nocodazole. Mitotic cells were specifically isolated by shake-off, and we found that the expression of *CDC25B*, *PLK1*, and *CCNB1* was reduced to a similar extent in both FoxM1 and VprBP-depleted cells relative to controls (Fig. S4B). We therefore conclude that VprBP activates the transcription of FoxM1 target genes during the G_2/M phase of the cell cycle.

FoxM1 has been implicated in mitotic entry and progression (6, 7). We examined the role of VprBP in cell cycle progression since its depletion reduces the expression of several FoxM1 target genes. U2OS cells were treated with either control or VprBP siRNAs and after 72 h were fixed and processed for phospho-histone H3 (P-H3) immunostaining to mark mitotic cells. Imaging was performed, and the percentage of P-H3-positive cells was determined. Eight percent of cells were in mitosis in control depleted populations (Fig. 4B). Depletion with two independent VprBP siRNAs significantly reduced the percentage of P-H3-positive mitotic cells, to 2.8% and 0.5% (Fig. 4B).

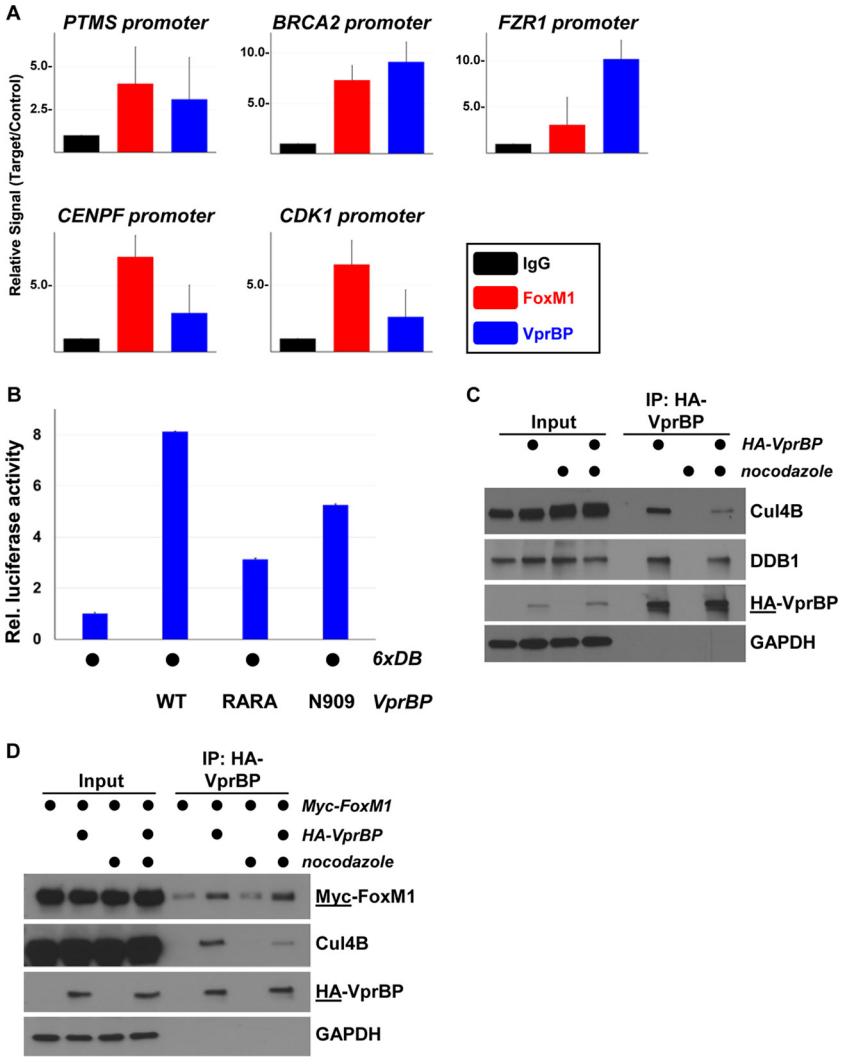

FIG 5 VprBP associates with FoxM1 promoters and activates independently from Cul4. (A) U2OS cells were synchronized in G_2/M phase and fixed for ChIP analysis with control IgG, FoxM1, and VprBP antibodies. VprBP associated with the promoters of some FoxM1 target genes. (B) $VprBP^{WT}$ and mutant versions that are impaired in binding DDB1 (RARA and N909) were expressed in 293T cells in combination with the 6×DB reporter. Luciferase activity was measured 48 h after transfection (error bars show standard deviations for technical triplicates). (C) HA-VprBP was transiently expressed in 293T cells that were subsequently treated with nocodazole or vehicle control (DMSO). VprBP was recovered on HA-agarose following lysis and analyzed by immunoblotting. (D) HA-VprBP and Myc-FoxM1 were transiently expressed in 293T cells that were subsequently treated with nocodazole or vehicle control (DMSO). VprBP was recovered on HA-agarose following lysis and analyzed by immunoblotting.

Thus, VprBP depletion blocks the accumulation of mitotic cell cycle genes and prevents M-phase entry, consistent with a role for VprBP in activating FoxM1.

We determined if VprBP localizes to the promoters of FoxM1 target genes, since it binds FoxM1 and regulates FoxM1 target gene expression. U2OS cells were synchronized in G_2/M phase and processed for chromatin immunoprecipitation (ChIP). Immunoprecipitation was performed in parallel with antibodies to control IgG, FoxM1, and VprBP. We detected an enrichment of both VprBP and FoxM1 at the promoters of previously characterized FoxM1 promoters, including *PTMS*, *BRCA2*, and *FZR1* (17). VprBP localized to a lesser extent to the FoxM1 targets *CENPF* and *CDK1* (Fig. 5A). Thus, FoxM1 and VprBP colocalize to FoxM1 target gene promoters.

Myc and ERα are activated by ubiquitylation via their respective ligases (26, 27, 57). We sought to gain similar mechanistic insight into the regulation of FoxM1 by VprBP. We determined if two independent versions of VprBP that are impaired in binding

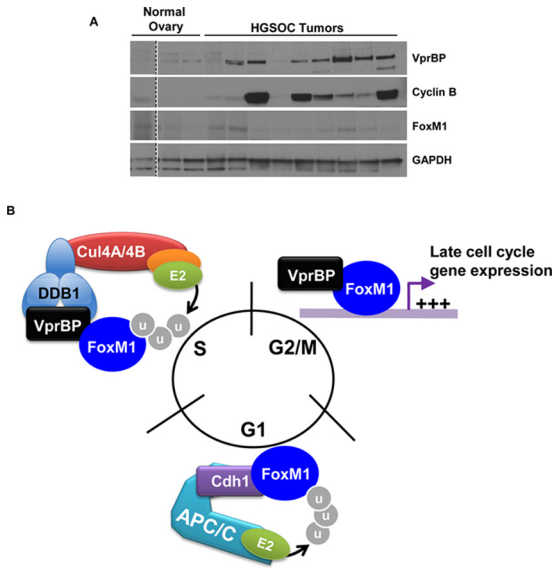

FIG 6 Implication in cell cycle control and malignancy. (A) Ovaries resected from patients with HGSOC were compared to normal ovaries by immunoblotting. (The dotted line indicates the splicing together of samples run on the same gel.) (B) Our data suggest that VprBP contributes to the degradation and activation of FoxM1. VprBP binds to the CRL4 ligase complex and targets FoxM1 for degradation during S phase. During G_2/M phases, when FoxM1 activity peaks, VprBP disengages from CRL4 and acts as a coactivator. FoxM1 is ubiquitylated and degraded by APC/C^{Cdh1} during G_1 phase.

DDB1 (N909 and RARA) are able to increase FoxM1 reporter activity (42). The 6×DB reporter activity was increased using an amino-terminal fragment of VprBP (N909) that cannot bind to the DDB1/Cul4 complex (Fig. 5B). Similar results were obtained with a mutant version of VprBP (RARA) that is also impaired in DDB1/Cul4 binding (Fig. 5B) (42). The response of 6×DB to $VprBP^{WT}$, $VprBP^{N909}$, and $VprBP^{RARA}$ is dose dependent (Fig. S4C). We conclude that VprBP activation of FoxM1 is independent of the CRL4 complex. These data also suggest that FoxM1 activation by VprBP is not due to a change in the abundance or stability of a secondary, unknown $CRL4^{VprBP}$ substrate.

We next asked if VprBP is still bound to Cul4B and DDB1 at a time in the cell cycle when FoxM1 is active. We introduced HA-VprBP into 293T cells that were then treated with either nocodazole or dimethyl sulfoxide (DMSO). Cells were lysed, and HA-VprBP immunoprecipitates were analyzed by immunoblotting. We found that the association of HA-VprBP with endogenous Cul4B, and to a lesser extent DDB1, was reduced in mitotic cells (Fig. 5C, lanes 6 versus 8). However, there was no change in the interaction between VprBP and FoxM1 in mitosis (Fig. 5C and D). Thus, VprBP association with the CRL4 complex is cell cycle regulated, and its partial dissociation coincides with the time at which FoxM1 is activated.

VprBP protein is upregulated in high-grade serous ovarian tumors. The FoxM1 gene expression signature is upregulated in ~90% of high-grade serous ovarian cancers (HGSOC) (12). However, the FoxM1 mRNA is overexpressed in only ~12% of tumors. To analyze the expression of VprBP in HGSOC tumors, we obtained surgically resected ovaries from HGSOC patients that had been histologically confirmed as serous ovarian cancer. As controls, we examined ovaries from women who underwent oophorectomy for reasons other than gynecological malignancy. FoxM1 levels were not elevated in HGSOC tumors relative to controls. Remarkably, VprBP protein was upregulated in seven of nine HGSOC tumors tested relative to control ovaries, where its levels were low or undetectable (Fig. 6A). Further, the well-established FoxM1 target cyclin B was expressed in six of the seven tumors in which VprBP was increased. *VPRBP* is not overexpressed at the mRNA level in HGSOC based on genomic analysis, suggesting that posttranscriptional mechanisms account for its overexpression (12).

DISCUSSION

Ubiquitylation has long been implicated as a key regulator of transcription and chromatin regulation in human cells. Ubiquitin was identified due to its conjugation to the core histone H2A and only later was identified by Hershko and colleagues as part of the intracellular protein degradation system (58). The yeast α-2 transcriptional repressor was one of the first identified *in vivo* targets of ubiquitin-dependent protein degradation (59). Ubiquitin has been best described for its role in inactivating target proteins through proteolysis. However, the emergence of complex ubiquitin chains of various topologies and the identification of their roles in various aspects of cellular physiology, besides protein degradation, illustrate the complex and sometimes paradoxical role that the ubiquitin machinery can play in signal transduction.

These multiple functions are evident in the role of ubiquitin signaling in transcriptional regulation. Interestingly, transcription factors and transcriptional coactivators can be activated by the ubiquitin machinery. For example, the transcriptional activation domain (TAD) of VP16 is activated in yeast by the SCF substrate receptor F-box protein, Met30 (29). Moreover, fusion of ubiquitin directly to VP16 restores its activity in the absence of Met30 without affecting VP16-TAD stability, providing an example of ubiquitin-dependent, degradation-independent transcriptional activation (29). There are also well-established examples of ubiquitin- and proteasome-dependent transcriptional activation in human cells. First is the Myc transcription factor. Myc degradation is controlled by the SCF (Skp2) E3 ubiquitin ligase, and Skp2 also promotes Myc transcriptional activation (26, 27). Consistently, a lysine-less version of Myc, which cannot be ubiquitylated and degraded with normal kinetics, still binds to the coactivator Max and localizes to target gene promoters but is unable to fully activate gene expression (28). Similarly, ERα is ubiquitylated and degraded in response to ligand (estrogen), and this is required for its full activation (30).

Here we show a FoxM1 activation mechanism that is ubiquitin and degradation independent yet involves a component of the ubiquitin system that can also regulate its destruction. We found that FoxM1 is a substrate of the $CRL4^{VprBP}$ E3 ubiquitin ligase. Analogous to Myc activation by Skp2, we discovered that VprBP potently activates FoxM1. However, the FoxM1 reporter was activated by two independent versions of VprBP that are impaired in binding to CRL4. Moreover, we demonstrate biochemically that VprBP is partially dissociated from the CRL4 complex at the time during the cell cycle when FoxM1 activity peaks. Together, these data suggest that FoxM1 activation by VprBP is ubiquitin and degradation independent. The ability of VprBP to activate FoxM1 independent of CRL4 binding provides a clear demonstration of E3 ligase substrate receptor repurposing. Moreover, it suggests the possibility that the activity of other CRL substrate receptors can be context dependent and dynamically altered by controlling their association with ubiquitin machinery.

We hypothesize that VprBP acts as a rheostat to control FoxM1 degradation and activation (Fig. 6). FoxM1 abundance is tightly controlled throughout the cell cycle by ubiquitylation. By tempering FoxM1 accumulation, VprBP could impair its activation. Late in the cell cycle, before mitosis, FoxM1 activity increases, contributing significantly to the expression of genes involved in mitotic entry and progression (9). At this time, the partial dissociation of VprBP from DDB1 and Cul4 (Fig. 5) would enhance its ability to activate FoxM1 (14). Consistent with this prediction, VprBP partially dissociates from CRL4 in mitosis and a mutant version of VprBP that is impaired for DDB1 binding can still activate FoxM1. Importantly, since VprBP depletion increases FoxM1 protein levels in mitotic cells, it is unlikely that VprBP acts through a switchlike mechanism, whereby it is either targeting FoxM1 for degradation or promoting its activation. In a rheostat model, VprBP could tune the output of FoxM1 by controlling both its activation and its degradation, with the relative role of each in a given cell determined by the extent of CRL4(VprBP) disassembly. It is interesting that VprBP is unique among CRL4 substrate receptors in that it is likely stoichiometrically bound to CRL4 (41, 60). In addition, VprBP

association with chromatin is tightly cell cycle regulated and occurs only at the time when FoxM1 is activated (G_2/M).

The mechanism by which VprBP dissociates from CRL4 remains unknown. We predict that posttranslational modification of VprBP could alter its chromatin association and/or binding to DDB1/Cul4. Alternatively, modification of DDB1 or Cul4 could regulate their association with VprBP. Modifications that affect FoxM1-VprBP binding cannot be ruled out, although they did not change in mitosis in our experiments. It is interesting that Chk2 phosphorylates FoxM1 in the same region as the one that we mapped as being important for VprBP binding (61) and Chk2 has been linked to mitotic progression (62). Dissecting the signaling pathways that control the relationship and interactions between VprBP, CRL4, and FoxM1 is an important area of future study.

FoxM1 is activated in a variety of human malignancies. Specifically, its transcriptional signature is upregulated in HGSOC, serous uterine cancer, and basal-like breast cancer (11–13). However, it is mechanistically unclear how FoxM1 is activated in each of these disease subtypes. Defects in ubiquitin signaling have been linked to changes in transcription factor stability in malignancies. This is illustrated by the regulation of p53 by Mdm2, as well as mutations FbxW7 that affect Myc. Unlike these two prominent examples, VprBP is neither significantly mutated nor transcriptionally altered in cancers in which the FoxM1 signature is upregulated. However, we show that VprBP is overexpressed at the protein level in HGSOC patient tumors. This suggests that VprBP might, in part, contribute to the FoxM1 expression signature observed in these cancers. It is important to note that cyclin B gene and other G_2/M genes can be controlled by multiple factors and FoxM1 itself is controlled by myriad mechanisms. Since VprBP is not overexpressed at the mRNA level based on transcriptomic analysis, it is presumably due to regulation of either its translation or its degradation. Cross talk between cell cycle E3 ligases is an emerging theme in cell cycle control (63), and perhaps VprBP stability is controlled by a second ubiquitin ligase.

MATERIALS AND METHODS

Immunoblot analysis. Cell extracts were prepared by lysis in ice-cold NETN buffer [20 mM Tris [pH 8.0], 100 mM NaCl, 0.5 mM EDTA, 0.5% NP-40, 1 mM 4-(2-aminoethyl)-benzenesulfonyl fluoride (AEBSF), 10 μg/ml leupeptin, 2 μg/ml aprotonin, 2 μg/ml pepstatin A]. Cells were lysed on ice for 15 min and then centrifuged at 14,000 rpm for 15 min at 4°C. Supernatant was collected, and protein concentrations were determined by the Bradford assay.

Tumor specimens were sampled from patients undergoing surgery for HGSOC at the University of North Carolina at Chapel Hill. The protocol was reviewed and exemption granted by the Institutional Review Board at the university. To extract protein from tissues, normal ovarian tissues and ovarian tumors were homogenized in ice-cold tissue homogenizing buffer (10 mM HEPES [pH 7.4], 50 mM β-glycerophosphate, 1% Triton X-100, 10% glycerol, 2 mM EDTA, 2 mM EGTA, 1 mM dithiothreitol [DTT], 10 mM NaF, 1 mM Na_3VO_4, 10 μg/ml leupeptin, 2 μg/ml aprotonin, 2 μg/ml pepstatin A, and 1 mM AEBSF) using TissueLyser II (Qiagen). The homogenates were placed on ice for 15 min and then centrifuged at 14,000 rpm for 15 min at 4°C. Supernatant was collected, and protein concentrations were determined by the Bradford assay.

For immunoblotting, samples were heated for 5 min at 95°C before electrophoresis. Samples were analyzed by SDS-PAGE using either homemade or Bio-Rad TGX gels, which were subsequently transferred onto nitrocellulose membranes (Bio-Rad). Membranes were blocked with 5% bovine serum albumin (BSA). Antibodies were incubated overnight, and signals were detected using Pierce ECL (Thermo Scientific). The primary antibodies used for immunoblot analysis, their sources, and the concentrations used are described in detail in the supplemental information. Secondary antibodies conjugated to horseradish peroxidase (HRP) were purchased from Jackson ImmunoResearch Laboratories.

Immunoprecipitation. Briefly, soluble protein extracts were prepared from HEK-293T cells transiently transfected with HA-VprBP and Myc-FoxM1 (wild type or mutants). Cells were lysed in NETN as described above. Precipitation was performed by rotating 50 μl of EZview Red anti-HA affinity gel or EZview Red anti-c-Myc affinity gel (Sigma) with 2 mg of soluble, clarified lysate overnight at 4°C. The affinity resin was recovered by centrifugation at 1,000 $\times$ *g* for 1 min and washed 3 times with ice-cold lysis buffer. Precipitates were eluted in SDS-PAGE buffer and analyzed by immunoblotting.

RT-qPCR. Total RNA was isolated with an RNeasy Plus minikit (Qiagen) and then reverse transcribed with a SuperScript III first-strand synthesis system (Invitrogen). The resulting cDNA was used for quantitative PCR with iTaq Universal SYBR green supermix (Bio-Rad). Data were normalized to GAPDH (glyceraldehyde-3-phosphate dehydrogenase). Real-time PCR and data collection were done with a QuantStudio 6 Flex real-time PCR system and software (Applied Biosystems). All of the primer sequences

used for RT-qPCR analysis, ChIP, and site-directed mutagenesis are described in the supplemental information.

Luciferase reporter assays. The FoxM1 6×DB luciferase reporter was a kind gift from Michael Whitfield (Dartmouth University). HEK-293T cells grown on 12-well plates were transiently transfected with 6 × DB reporter in combination with different constructs (FoxM1, MELK, and VprBP) using PolyJet Plus transfection reagent (SignaGen Laboratories). The MELK expression vector was a kind gift from Lee Graves (University of North Carolina). The Nrf2 expression vector and Nrf2 luciferase reporter were gifts from Ben Major (University of North Carolina). VprBP expression vectors were a kind gift from Yue Xiong (University of North Carolina). Cells were routinely collected at 48 h posttransfection. Luciferase activity was measured using the luciferase reporter assay system (Promega). Experiments were performed in three technical replicates each. Statistical differences were determined using Student's *t* test.

Flow cytometry. For cell cycle profiling, trypsinized cells were washed with phosphate-buffered saline (PBS), fixed in cold 70% ethanol, and stored overnight at −20°C. DNA was stained for 30 min in 25 μg/ml propidium iodide and 100 μg/ml RNase. Samples were analyzed using a CyAn flow cytometer (Beckman Coulter) and FlowJo software.

***In vivo* ubiquitination assay.** HEK-293T cells were cotransfected with 6His-ubiquitin and HA-VprBP, with or without Myc-FoxM1. Forty-eight hours after transfection, cells were lysed in denaturing buffer, mixed, and sonicated. Samples were incubated with equilibrated HisPur Ni-NTA Resin (ThermoFisher) overnight at 4°C on a rotator. After repeated washing, the resin was eluted with SDS-PAGE sample buffer. Detailed experimental procedures describing the wash and lysis buffers are described in reference 64.

Expression and binding assay for VprBP and FoxM1. VprBP was expressed from pcDNA3 using the PURExpress system supplemented with [^{35}S]methionine according to the manufacturer protocol. Full-length FoxM1c (aa 1 to 763) was subcloned into pET-28b, producing a C-terminally 6×His-tagged clone, and expressed in *Escherichia coli* BL21(DE3) cells. Protein expression was induced with isopropyl-β-D-thiogalactopyranoside (IPTG; 250 μM) at 17°C for 18 h. The pellet was sonicated in 40 ml of lysis buffer [20 mM KH_2PO_4 (pH 7.5), 500 mM NaCl, 10 mM imidazole, 1 mM Tris(2-carboxyethyl)phosphine (TCEP), 10% glycerol, 2 mM phenylmethylsulfonyl fluoride (PMSF), 1 protease tablet, 5 mM $MgCl_2$, 40 units of DNase I]. Lysis supernatant was loaded on a 5-ml HisTrap HP column, washed with buffer A (20 mM KH_2PO_4 [pH 7.5], 500 mM NaCl, 10 mM imidazole, 1 mM TCEP, 10% glycerol), and eluted with buffer B (20 mM KH_2PO_4 [pH 7.5], 500 mM NaCl, 500 mM imidazole, 1 mM TCEP, 10% glycerol). Protein fractions were pooled and desalted with a 200-ml HiPrep 26/10 column into buffer C (20 mM KH_2PO_4 [pH 7.5], 200 mM NaCl, 10 mM imidazole, 1 mM TCEP).

Nickel-nitrilotriacetic acid (Ni-NTA) resin was prepared with wash buffer (20 mM KH_2PO_4 [pH 7.5], 200 mM NaCl, 10 mM imidazole, 1 mM TCEP, 0.002% Tween 20) and loaded with FoxM1c-6His. The column was washed with 3 column volumes of wash buffer, and purified VprBP was added to the resin for 1 h at 4°C. The resin was washed and eluted (using 20 mM KH_2PO_4 [pH 7.5], 200 mM NaCl, 500 mM imidazole, 1 mM TCEP, 0.002% Tween 20) at 75°C, and samples were visualized by autoradiography.

SUPPLEMENTAL MATERIAL

Supplemental material for this article may be found at https://doi.org/10.1128/MCB.00609-16.

SUPPLEMENTAL FILE 1, PDF file, 0.4 MB.

ACKNOWLEDGMENTS

Thanks go to David Allison and Greg Wang (UNC—Chapel Hill) for assistance with ChIP experiments and the following individuals for reagents (see Materials and Methods for details): Yue Xiong (UNC—Chapel Hill), Lee Graves (UNC—Chapel Hill), Ben Major (UNC—Chapel Hill), Anja Bielinsky (University of Minnesota), and Mike Whitfield (Dartmouth University). We acknowledge the UNC Flow Cytometry Core Facility (supported in part by P30 CA016086 Cancer Center Core Support Grant to the Lineberger Cancer Center).

The Emanuele lab is supported by start-up funds from UNC (University Cancer Research Fund) and grants from the Susan G. Komen Foundation (CCR14298820), the Jimmy-V Foundation, and the National Institutes of Health (R01GM120309).

We declare that we have no competing financial interests related to this work.

Author contributions are as follows. M.J.E. conceived of and designed experiments. X.W. helped design and carried out the vast majority of the cell biological experiments. A.A. performed cell cycle assays and aided in qPCR analysis. C.A.M., J.L.K., and R.C. contributed experimentally to the cell biology aspects of this work. K.B. and A.B. performed *in vitro* binding assays. V.B.-J. and C.Z. coordinated the procurement of tissue samples.

REFERENCES

1. Allis CD, Jenuwein T. 2016. The molecular hallmarks of epigenetic control. Nat Rev Genet 17:487–500. https://doi.org/10.1038/nrg.2016.59.
2. Ye H, Kelly TF, Samadani U, Lim L, Rubio S, Overdier DG, Roebuck KA, Costa RH. 1997. Hepatocyte nuclear factor 3/fork head homolog 11 is expressed in proliferating epithelial and mesenchymal cells of embryonic and adult tissues. Mol Cell Biol 17:1626–1641. https://doi.org/10.1128/MCB.17.3.1626.
3. Ye H, Holterman AIX, Yoo KW, Franks RR, Costa RH. 1999. Premature expression of the winged helix transcription factor HFH-11B in regenerating mouse liver accelerates hepatocyte entry into S phase. Mol Cell Biol 19:8570–8580. https://doi.org/10.1128/MCB.19.12.8570.
4. Korver W, Roose J, Clevers H. 1997. The winged-helix transcription factor Trident is expressed in cycling cells. Nucleic Acids Res 25:1715–1719. https://doi.org/10.1093/nar/25.9.1715.
5. Bella L, Zona S, Nestal de Moraes G, Lam EWF. 2014. FOXM1: a key oncofoetal transcription factor in health and disease. Semin Cancer Biol 29:32–39. https://doi.org/10.1016/j.semcancer.2014.07.008.
6. Laoukili J, Kooistra MRH, Brás A, Kauw J, Kerkhoven RM, Morrison A, Clevers H, Medema RH. 2005. FoxM1 is required for execution of the mitotic programme and chromosome stability. Nat Cell Biol 7:126–136. https://doi.org/10.1038/ncb1217.
7. Schüller U, Zhao Q, Godinho SA, Heine VM, Medema RH, Pellman D, Rowitch DH. 2007. Forkhead transcription factor FoxM1 regulates mitotic entry and prevents spindle defects in cerebellar granule neuron precursors. Mol Cell Biol 27:8259–8270. https://doi.org/10.1128/MCB.00707-07.
8. Krupczak-Hollis K, Wang X, Kalinichenko VV, Gusarova GA, Wang IC, Dennewitz MB, Yoder HM, Kiyokawa H, Kaestner KH, Costa RH. 2004. The mouse Forkhead Box m1 transcription factor is essential for hepatoblast mitosis and development of intrahepatic bile ducts and vessels during liver morphogenesis. Dev Biol 276:74–88. https://doi.org/10.1016/j.ydbio.2004.08.022.
9. Grant GD, Brooks L, Zhang X, Mahoney JM, Martyanov V, Wood TA, Sherlock G, Cheng C, Whitfield ML. 2013. Identification of cell cycle-regulated genes periodically expressed in U2OS cells and their regulation by FOXM1 and E2F transcription factors. Mol Biol Cell 24:3634–3650. https://doi.org/10.1091/mbc.E13-05-0264.
10. Halasi M, Gartel AL. 2013. Targeting FOXM1 in cancer. Biochem Pharmacol 85:644–652. https://doi.org/10.1016/j.bcp.2012.10.013.
11. Cancer Genome Atlas Network. 2012. Comprehensive molecular portraits of human breast tumours. Nature 490:61–70. https://doi.org/10.1038/nature11412.
12. Cancer Genome Atlas Research Network. 2011. Integrated genomic analyses of ovarian carcinoma. Nature 474:609–615. https://doi.org/10.1038/nature10166.
13. Cancer Genome Atlas Research Network, Kandoth C, Schultz N, Cherniack AD, Akbani R, Liu Y, Shen H, Robertson A, G, Pashtan I, Shen R, Benz CC, Yau C, Laird PW, Ding L, Zhang W, Mills GB, Kucherlapati R, Mardis ER, Levine DA. 2013. Integrated genomic characterization of endometrial carcinoma. Nature 497:67–73. https://doi.org/10.1038/nature12113.
14. Grant GD, Gamsby J, Martyanov V, Brooks L, George LK, Mahoney JM, Loros JJ, Dunlap JC, Whitfield ML. 2012. Live-cell monitoring of periodic gene expression in synchronous human cells identifies Forkhead genes involved in cell cycle control. Mol Biol Cell 23:3079–3093. https://doi.org/10.1091/mbc.E11-02-0170.
15. Wang I, Chen Y, Hughes D, Petrovic V, Major ML, Park HJ, Tan Y, Ackerson T, Costa RH. 2005. Forkhead box M1 regulates the transcriptional network of genes essential for mitotic progression and genes encoding the SCF (Skp2-Cks1) ubiquitin ligase. Mol Cell Biol 25:10875–10894. https://doi.org/10.1128/MCB.25.24.10875-10894.2005.
16. Sadasivam S, Duan S, DeCaprio JA. 2012. The MuvB complex sequentially recruits B-Myb and FoxM1 to promote mitotic gene expression. Genes Dev 26:474–489. https://doi.org/10.1101/gad.181933.111.
17. Chen X, Quaas M, Fischer M, Han N, Stutchbury B, Sharrocks AD, Engeland K. 2013. The Forkhead transcription factor FOXM1 controls cell cycle-dependent gene expression through an atypical chromatin binding mechanism. Mol Cell Biol 33:227–236. https://doi.org/10.1128/MCB.00881-12.
18. Sanders DA, Gormally MV, Marsico G, Beraldi D, Tannahill D, Balasubramanian S. 2015. FOXM1 binds directly to non-consensus sequences in the human genome. Genome Biol 16:130. https://doi.org/10.1186/s13059-015-0696-z.
19. Park HJ, Wang Z, Costa RH, Tyner A, Lau LF, Raychaudhuri P. 2008. An N-terminal inhibitory domain modulates activity of FoxM1 during cell cycle. Oncogene 27:1696–1704. https://doi.org/10.1038/sj.onc.1210814.
20. Fu Z, Malureanu L, Huang J, Wang W, Li H, van Deursen JM, Tindall DJ, Chen J. 2008. Plk1-dependent phosphorylation of FoxM1 regulates a transcriptional programme required for mitotic progression. Nat Cell Biol 10:1076–1082. https://doi.org/10.1038/ncb1767.
21. Zhang J, Yuan C, Wu J, Elsayed Z, Fu Z. 2015. Polo-like kinase 1-mediated phosphorylation of Forkhead box protein M1b antagonizes its SUMOylation and facilitates its mitotic function. J Biol Chem 290:3708–3719. https://doi.org/10.1074/jbc.M114.634386.
22. Laoukili J, Alvarez M, Meijer LA, Stahl M, Mohammed S, Kleij L, Heck AJR, Medema RH. 2008. Activation of FoxM1 during G2 requires cyclin A/Cdk-dependent relief of autorepression by the FoxM1 N-terminal domain. Mol Cell Biol 28:3076–3087. https://doi.org/10.1128/MCB.01710-07.
23. Major ML, Lepe R, Costa RH. 2004. Forkhead box M1B transcriptional activity requires binding of Cdk-cyclin complexes for phosphorylation-dependent recruitment of p300/CBP coactivators. Mol Cell Biol 24:2649–2661. https://doi.org/10.1128/MCB.24.7.2649-2661.2004.
24. Joshi K, Banasavadi-Siddegowda Y, Mo X, Kim SH, Mao P, Kig C, Nardini D, Sobol RW, Chow LML, Kornblum HI, Waclaw R, Beullens M, Nakano I. 2013. MELK-dependent FOXM1 phosphorylation is essential for proliferation of glioma stem cells. Stem Cells 31:1051–1063. https://doi.org/10.1002/stem.1358.
25. Geng F, Wenzel S, Tansey WP. 2012. Ubiquitin and proteasomes in transcription. Annu Rev Biochem 81:177–201. https://doi.org/10.1146/annurev-biochem-052110-120012.
26. Kim SY, Herbst A, Tworkowski KA, Salghetti SE, Tansey WP. 2003. Skp2 regulates Myc protein stability and activity. Mol Cell 11:1177–1188. https://doi.org/10.1016/S1097-2765(03)00173-4.
27. von der Lehr N, Johansson S, Wu S, Bahram F, Castell A, Cetinkaya C, Hydbring P, Weidung I, Nakayama K, Nakayama KI, Söderberg O, Kerppola TK, Larsson LG. 2003. The F-box protein Skp2 participates in c-Myc proteosomal degradation and acts as a cofactor for c-Myc-regulated transcription. Mol Cell 11:1189–1200. https://doi.org/10.1016/S1097-2765(03)00193-X.
28. Jaenicke LA, von Eyss B, Carstensen A, Wolf E, Xu W, Greifenberg AK, Geyer M, Eilers M, Popov N. 2016. Ubiquitin-dependent turnover of MYC antagonizes MYC/PAF1C complex accumulation to drive transcriptional elongation. Mol Cell 61:54–67. https://doi.org/10.1016/j.molcel.2015.11.007.
29. Salghetti SE, Caudy AA, Chenoweth JG, Tansey WP. 2001. Regulation of transcriptional activation domain function by ubiquitin. Science 293:1651–1653. https://doi.org/10.1126/science.1062079.
30. Reid G, Hübner MR, Métivier R, Brand H, Denger S, Manu D, Beaudouin J, Ellenberg J, Gannon F. 2003. Cyclic, proteasome-mediated turnover of unliganded and liganded ERalpha on responsive promoters is an integral feature of estrogen signaling. Mol Cell 11:695–707. https://doi.org/10.1016/S1097-2765(03)00090-X.
31. Lonard DM, Nawaz Z, Smith CL, O'Malley BW. 2000. The 26S proteasome is required for estrogen receptor-alpha and coactivator turnover and for efficient estrogen receptor-alpha transactivation. Mol Cell 5:939–948. https://doi.org/10.1016/S1097-2765(00)80259-2.
32. Wu RC, Feng Q, Lonard DM, O'Malley BW. 2007. SRC-3 coactivator functional lifetime is regulated by a phospho-dependent ubiquitin time clock. Cell 129:1125–1140. https://doi.org/10.1016/j.cell.2007.04.039.
33. Emanuele MJ, Elia AEH, Xu Q, Thoma CR, Izhar L, Leng Y, Guo A, Chen Y-N, Rush J, Hsu PW, Yen H-CS, Elledge SJ. 2011. Global identification of modular cullin-RING ligase substrates. Cell 147:459–474. https://doi.org/10.1016/j.cell.2011.09.019.
34. Jackson S, Xiong Y. 2009. CRL4s: the CUL4-RING E3 ubiquitin ligases. Trends Biochem Sci 34:562–570. https://doi.org/10.1016/j.tibs.2009.07.002.
35. Guerrero-Santoro J, Kapetanaki MG, Hsieh CL, Gorbachinsky I, Levine AS, Rapić-Otrin V. 2008. The cullin 4B-based UV-damaged DNA-binding protein ligase binds to UV-damaged chromatin and ubiquitinates histone H2A. Cancer Res 68:5014–5022. https://doi.org/10.1158/0008-5472.CAN-07-6162.
36. Jin J, Arias EE, Chen J, Harper JW, Walter JC. 2006. A family of diverse Cul4-Ddb1-interacting proteins includes Cdt2, which is required for S phase destruction of the replication factor Cdt1. Mol Cell 23:709–721. https://doi.org/10.1016/j.molcel.2006.08.010.
37. Angers S, Li T, Yi X, MacCoss MJ, Moon RT, Zheng N. 2006. Molecular

architecture and assembly of the DDB1-CUL4A ubiquitin ligase machinery. Nature 443:590–593.
38. He YJ, McCall CM, Hu J, Zeng Y, Xiong Y. 2006. DDB1 functions as a linker to recruit receptor WD40 proteins to CUL4-ROC1 ubiquitin ligases. Genes Dev 20:2949–2954. https://doi.org/10.1101/gad.1483206.
39. Zhang S, Feng Y, Narayan O, Zhao LJ. 2001. Cytoplasmic retention of HIV-1 regulatory protein Vpr by protein-protein interaction with a novel human cytoplasmic protein VprBP. Gene 263:131–140. https://doi.org/10.1016/S0378-1119(00)00583-7.
40. Andersen JL, Le Rouzic E, Planelles V. 2008. HIV-1 Vpr: mechanisms of G2 arrest and apoptosis. Exp Mol Pathol 85:2–10. https://doi.org/10.1016/j.yexmp.2008.03.015.
41. McCall CM, Miliani de Marval PL, Chastain PD, Jackson SC, He YJ, Kotake Y, Cook JG, Xiong Y. 2008. Human immunodeficiency virus type 1 Vpr-binding protein VprBP, a WD40 protein associated with the DDB1-CUL4 E3 ubiquitin ligase, is essential for DNA replication and embryonic development. Mol Cell Biol 28:5621–5633. https://doi.org/10.1128/MCB.00232-08.
42. Nakagawa T, Lv L, Nakagawa M, Yu Y, Yu C, D'Alessio AC, Nakayama K, Fan H-Y, Chen X, Xiong Y. 2015. CRL4(VprBP) E3 ligase promotes monoubiquitylation and chromatin binding of TET dioxygenases. Mol Cell 57:247–260. https://doi.org/10.1016/j.molcel.2014.12.002.
43. Kaur M, Khan MM, Kar A, Sharma A, Saxena S. 2012. CRL4-DDB1-VPRBP ubiquitin ligase mediates the stress triggered proteolysis of Mcm10. Nucleic Acids Res 40:7332–7346. https://doi.org/10.1093/nar/gks366.
44. Hrecka K, Hao C, Gierszewska M, Swanson SK, Kesik-Brodacka M, Srivastava S, Florens L, Washburn MP, Skowronski J. 2011. Vpx relieves inhibition of HIV-1 infection of macrophages mediated by the SAMHD1 protein. Nature 474:658–661. https://doi.org/10.1038/nature10195.
45. Li W, You L, Cooper J, Schiavon G, Pepe-Caprio A, Zhou L, Ishii R, Giovannini M, Hanemann CO, Long SB, Erdjument-Bromage H, Zhou P, Tempst P, Giancotti FG. 2010. Merlin/NF2 suppresses tumorigenesis by inhibiting the E3 ubiquitin ligase CRL4(DCAF1) in the nucleus. Cell 140:477–490. https://doi.org/10.1016/j.cell.2010.01.029.
46. Yen H-CS, Xu Q, Chou DM, Zhao Z, Elledge SJ. 2008. Global protein stability profiling in mammalian cells. Science 322:918–923. https://doi.org/10.1126/science.1160489.
47. Soucy TA, Smith PG, Milhollen MA, Berger AJ, Gavin JM, Adhikari S, Brownell JE, Burke KE, Cardin DP, Critchley S, Cullis CA, Doucette A, Garnsey JJ, Gaulin JL, Gershman RE, Lublinsky AR, McDonald A, Mizutani H, Narayanan U, Olhava EJ, Peluso S, Rezaei M, Sintchak MD, Talreja T, Thomas MP, Traore T, Vyskocil S, Weatherhead GS, Yu J, Zhang J, Dick LR, Claiborne CF, Rolfe M, Bolen JB, Langston SP. 2009. An inhibitor of NEDD8-activating enzyme as a new approach to treat cancer. Nature 458:732–736. https://doi.org/10.1038/nature07884.
48. Havens CG, Walter JC. 2009. Docking of a specialized PIP Box onto chromatin-bound PCNA creates a degron for the ubiquitin ligase CRL4Cdt2. Mol Cell 35:93–104. https://doi.org/10.1016/j.molcel.2009.05.012.
49. Park HJ, Costa RH, Lau LF, Tyner AL, Raychaudhuri P. 2008. Anaphase-promoting complex/cyclosome-CDH1-mediated proteolysis of the forkhead box M1 transcription factor is critical for regulated entry into S phase. Mol Cell Biol 28:5162–5171. https://doi.org/10.1128/MCB.00387-08.
50. Laoukili J, Alvarez-Fernandez M, Stahl M, Medema RH. 2008. FoxM1 is degraded at mitotic exit in a Cdh1-dependent manner. Cell Cycle 7:2720–2726. https://doi.org/10.4161/cc.7.17.6580.
51. Kruiswijk F, Yuniati L, Magliozzi R, Low TY, Lim R, Bolder R, Mohammed S, Proud CG, Heck AJR, Pagano M, Guardavaccaro D. 2012. Coupled activation and degradation of eEF2K regulates protein synthesis in response to genotoxic stress. Sci Signal 5:ra40. https://doi.org/10.1126/scisignal.2002718.
52. Goldberg AL, St John AC. 1976. Intracellular protein degradation in mammalian and bacterial cells. Part 2. Annu Rev Biochem 45:747–803. https://doi.org/10.1146/annurev.bi.45.070176.003531.
53. Tan M-KM, Lim H-J, Bennett EJ, Shi Y, Harper JW. 2013. Parallel SCF adaptor capture proteomics reveals a role for SCFFBXL17 in NRF2 activation via BACH1 repressor turnover. Mol Cell 52:9–24. https://doi.org/10.1016/j.molcel.2013.08.018.
54. Kim TY, Siesser PF, Rossman KL, Goldfarb D, Mackinnon K, Yan F, Yi X, MacCoss MJ, Moon RT, Der CJ, Major MB. 2015. Substrate trapping proteomics reveals targets of the βTrCP2/FBXW11 ubiquitin ligase. Mol Cell Biol 35:167–181. https://doi.org/10.1128/MCB.00857-14.
55. Schwefel D, Groom HCT, Boucherit VC, Christodoulou E, Walker PA, Stoye JP, Bishop KN, Taylor IA. 2014. Structural basis of lentiviral subversion of a cellular protein degradation pathway. Nature 505:234–238. https://doi.org/10.1038/nature12815.
56. Ahn J, Hao C, Yan J, DeLucia M, Mehrens J, Wang C, Gronenborn AM, Skowronski J. 2012. HIV/simian immunodeficiency virus (SIV) accessory virulence factor Vpx loads the host cell restriction factor SAMHD1 onto the E3 ubiquitin ligase complex CRL4DCAF1. J Biol Chem 287:12550–12558. https://doi.org/10.1074/jbc.M112.340711.
57. Nawaz Z, Lonard DM, Dennis AP, Smith CL, O'Malley BW. 1999. Proteasome-dependent degradation of the human estrogen receptor. Proc Natl Acad Sci U S A 96:1858–1862. https://doi.org/10.1073/pnas.96.5.1858.
58. Varshavsky A. 2006. The early history of the ubiquitin field. Protein Sci 15:647–654. https://doi.org/10.1110/ps.052012306.
59. Hochstrasser M, Varshavsky A. 1990. In vivo degradation of a transcriptional regulator: the yeast alpha 2 repressor. Cell 61:697–708. https://doi.org/10.1016/0092-8674(90)90481-S.
60. Bennett EJ, Rush J, Gygi SP, Harper JW. 2010. Dynamics of cullin-RING ubiquitin ligase network revealed by systematic quantitative proteomics. Cell 143:951–965. https://doi.org/10.1016/j.cell.2010.11.017.
61. Tan Y, Raychaudhuri P, Costa RH. 2007. Chk2 mediates stabilization of the FoxM1 transcription factor to stimulate expression of DNA repair genes. Mol Cell Biol 27:1007–1016. https://doi.org/10.1128/MCB.01068-06.
62. Stolz A, Ertych N, Kienitz A, Vogel C, Schneider V, Fritz B, Jacob R, Dittmar G, Weichert W, Petersen I, Bastians H. 2010. The CHK2–BRCA1 tumour suppressor pathway ensures chromosomal stability in human somatic cells. Nat Cell Biol 12:492–499. https://doi.org/10.1038/ncb2051.
63. Choudhury R, Bonacci T, Arceci A, Lahiri D, Mills CA, Kernan JL, Branigan TB, DeCaprio JA, Burke DJ, Emanuele MJ. 2016. APC/C and SCF(cyclin F) constitute a reciprocal feedback circuit controlling S-phase entry. Cell Rep 16:3359–3372. https://doi.org/10.1016/j.celrep.2016.08.058.
64. Bonacci T, Audebert S, Camoin L, Baudelet E, Bidaut G, Garcia M, Witzel II, Perkins ND, Borg JP, Iovanna JL, Soubeyran P. 2014. Identification of new mechanisms of cellular response to chemotherapy by tracking changes in post-translational modifications by ubiquitin and ubiquitin-like proteins. J Proteome Res 13:2478–2494. https://doi.org/10.1021/pr401258d.